Anal Bioanal Chem (2015) 407:8087–8095
DOI 10.1007/s00216-015-8982-x

RESEARCH PAPER

Preparation of molecularly imprinted polymer coated quantum dots to detect nicosulfuron in water samples

Xiaohui Ren[1] · **Ligang Chen**[1]

Received: 1 July 2015 / Revised: 30 July 2015 / Accepted: 13 August 2015 / Published online: 25 August 2015

Abstract A novel dual-function material was synthesized by anchoring a molecularly imprinted polymer (MIP) layer on Mn-doped ZnS quantum dots (QDs) via a sol–gel process using 3-aminopropyltriethoxysilane (APTES) as a functional monomer, tetraethoxysilane (TEOS) as cross-linker, and nicosulfuron as template through a surface imprinting method. The amino groups in the APTES interact with the functional groups in the template molecules to form a complex through hydrogen bonding. The energy of the QDs was transferred to the complex, resulting in the quenching of the QDs and thus decreasing the fluorescence intensity, which allowed the nicosulfuron to be sensed optically. Fluorescence intensity from MIP-coated QDs was more strongly quenched by nicosulfuron than that of the non-imprinted polymer, which indicated that the MIP-coated QDs which acted as a fluorescence probe could selectively recognize nicosulfuron. Under the optimal conditions, it can detect down to 1.1 nmol L^{-1} of nicosulfuron, and a linear relationship has been obtained covering the concentration range of 12–6000 nmol L^{-1}. The recoveries were in the range from 89.6 to 96.5 %, and the relative standard deviations were in the range of 2.5–5.7 %. The present study established a new strategy to combine inorganic (Mn-doped ZnS QDs)-organic MIPs, which is successfully applied to determine nicosulfuron in water samples.

Keywords Molecular imprinting · Quantum dots · Fluorescence quenching · Nicosulfuron

Introduction

Molecular imprinting emerged as a powerful technique for preparation of polymeric materials with high recognition ability and has attracted tremendous research interest from scientists engaged in sensor development due to their unique properties, such as high selectivity, physical robustness, thermal stability, as well as low cost and easy preparation [1–3]. Molecularly imprinted polymers (MIPs) are synthetic polymers with specific cavities designed for template molecules [4]. Because of its imprinting according to the size, shape, and functional groups of a template molecule, MIPs act as an artificial specific receptor [5]. Their binding mechanism is similar to the "key-lock" principle of enzymes, thereby allowing high affinity and specificity for its template [6]. Generally, there are three binding interactions between template and monomers such as covalent, non-covalent, and semi-covalent [7]. Most of the used monomers are commercially available, and they exhibit excellent mechanical and chemical stability, high binding affinity, and selective target recognition ability [8]. After the template removed, specific cavities were left that can selectively rebind template molecules in size, shape, and functional groups [9]. In addition, the high selectivity of MIPs, their simplicity of production, and less strict operation conditions compared to immunosorbents make their applications remarkably widespread.

In recent years, quantum dots (QDs) have been widespread which was caused by their unique optical and electronic properties. QDs have large surface-to-volume ratio and confinement effect [10]. QDs have proved to be promising in a number of applications in many scopes such as sensors [11], solar

Electronic supplementary material The online version of this article (doi:10.1007/s00216-015-8982-x) contains supplementary material, which is available to authorized users.

✉ Ligang Chen
ligangchen2010@aliyun.com

[1] Department of Chemistry, College of Science, Northeast Forestry University, 26 Hexing Road, Harbin 150040, China

cells [12], lasers [13], light emitting diodes [14], and biological imaging [15]. QDs have been used to sense and recognize the organic and inorganic compounds in environment [16]. They have some advantages, such as good photostability, bright photoluminescence, narrow emission, broad excitation, high quantum yields, and large Stokes shift [17, 18]. Most of the experimentally studied and commercial QDs are synthesized via traditional organometallic methods, which contain highly toxic elements, such as cadmium, lead, and mercury, and use organic solvents and ligands at high temperatures [19]. In recent years, the emphasis has shifted toward the fabrication of non-cadmium-based QDs. Out of various II–VI semiconductor QDs, ZnS has attracted a lot of attentions due to its wide direct band gap (3.67 eV at room temperature for cubic phase ZnS), large exciton binding energy (~40 meV), and its potential application. With Mn^{2+} as the dopant, Mn^{2+} ions incorporated into ZnS nanocrystals act as luminescence centers. The orange emission observed at 595 nm originates from the $^4T_1 \rightarrow {}^6A_1$ transition of the Mn^{2+} ions on Zn^{2+} sites, where Mn^{2+} is tetrahedrally coordinated by S^{2-} [20]. Moreover, coating the surface of these semiconductor nanoparticles with suitable ligands or capping agents has profound effects on the photoluminescence response of the QDs to some chemical species [21].

Nicosulfuron composed of a sulphonyl structure linked to a urea group which belongs to sulfonylurea herbicides. The structure of nicosulfuron was shown in Fig. S1 (see Electronic Supplementary Material (ESM)). Sulfonylurea herbicides, discovered in the mid-1970s, are a class of low-application-rate herbicides increasingly used for the control of broad-leaved weeds and some grasses in cereals and other row crops owing to their high herbicidal activity [22]. However, these economic benefits are not without risk to human health and environmental damage. They have toxicity and potential adverse influence on ecosystem which exist in the center of health and safety consideration [23]. In addition, due to their high solubility in water, moderate to high mobility, and slow degradation, they are being detected in surface and groundwater [24]. They have other defects, such as chemical and thermal instability. Because of these defects, it is an important challenge to establish a simple detection method for these compounds in environmental samples [23].

Analytical methods such as high-performance liquid chromatography (HPLC) [23], liquid chromatography–mass spectrophotometry (LC–MS) [25], and gas chromatrography (GC) [26] have been developed for the determination of herbicides. Although these methods show promising results for sensitive detection of herbicides, there are still some hindrances including sophisticated instrumentation, extensive sample preparation, and the need for highly skilled personnel. Therefore, it is necessary to determine herbicides in environmental samples with a simple and effective method.

In this work, a simple procedure was developed to synthesize MIP-coated QDs as a probe material by using nicosulfuron as a template molecule. Fluorescence spectrophotometer, Fourier transform infrared spectroscopy (FT-IR), transmission electron microscope (TEM), and X-ray powder diffraction (XRD) were applied to the characterization of MIP-coated QDs. The response of fluorescence intensity and the application capability of the developed molecularly imprinted probe material were fully evaluated in a series of experiments, and the possible mechanism was discussed. Then, the MIP-coated QDs were used as fluorescence probe to offer a convenient, rapid, and accurate determination proposal.

Experimental

Samples and reagents

The standards of nicosulfuron and chlorimuron-ethyl were obtained from Sigma-Aldrich (St. Louis, MO, USA). Zinc sulfate heptahydrate ($ZnSO_4 \cdot 7H_2O$) was obtained from Shuangchuan (Tianjin, China). Manganese (II) chloride tetrahydrate ($MnCl_2 \cdot 4H_2O$) was obtained from Bodi (Tianjin, China). Sodium sulfide ($Na_2S \cdot 9H_2O$) was obtained from Kaitong (Tianjin, China). L-Cysteine was purchased from Energy Chemical (Shanghai, China). 3-Aminopropyltriethoxysilane (APTES) was obtained from Aladdin (Shanghai, China). Ammonium hydroxide ($NH_3 \cdot H_2O$, 25 %) was obtained from Guangfu (Tianjin, China). Tetraethoxysilane (TEOS), ethanol, methanol, acetic acid (CH_3COOH), and sodium hydroxide (NaOH) were purchased from Kermel (Tianjin, China). All chemicals employed in this study were of analytical grade. High-purity water was obtained from a Milli-Q water system (Millipore, Billerica, MA, USA).

Nicosulfuron was dissolved in methanol to prepare the stock solution (2.5 mmol L^{-1}), which was stored in dark condition at 4 °C. The working solutions were prepared daily by diluting the stock solution.

Three river water samples were collected from Harbin (China). All water samples were stored in a refrigerator at 4 °C. The pH of river water samples was in a range of 6.5–7.5.

Apparatus

Fourier transform infrared (FT-IR) 360 spectrometer (Nicolet, Madison, WI, USA) was used for the characterization of functional groups of MIP-coated QDs. The X-ray diffraction (XRD) spectrum was collected on a Shimadzu XRD-600 diffractometer (Kyoto, Japan) with Cu Kα radiation. The morphology of MIP-coated QDs was observed with a transmission electron microscope (TEM) (H7650, Hitachi, Japan). UV spectrum was recorded on TU-1901 spectrometer (PERSEE, Beijing, China). The size of QDs and MIP-coated QDs was observed with Malvern Zetasizer model Nano ZS90 (Malvern, England). Fluorescence intensity studies were carried out at

room temperature by using F-4600 fluorescence spectrophotometer (Hitachi, Japan) which was equipped with a plotter unit and a quartz cell. A KQ5200E ultrasonic apparatus (Kunshan Instrument, Kunshan, China) was used for making samples dispersed evenly.

Synthesis of MIP-coated QDs

The synthesis process of MIP-coated QDs involves two major steps: synthesis of Mn-doped ZnS QDs is the first step, and the surface imprinting of polymers onto modified Mn-doped ZnS QDs is the second step.

The synthesis method of Mn-doped ZnS QDs was shown as follows. At first, 25 mmol of $ZnSO_4 \cdot 7H_2O$, 2 mmol of $MnCl_2 \cdot 4H_2O$, and 80 mL of water were kept stirring for 20 min under the protection of nitrogen gas. Then, 10 mL, 25 mmol $Na_2S \cdot 9H_2O$ solution was added drop into the mixture [27]. After stirred for 30 min, 10 mL, 1.25 mmol L-cysteine solution was added for modifying the Mn-doped ZnS QDs. The pH value of the solution was adjusted to 11.0 with 1.0 mol L^{-1} NaOH. After stirred for 20 h, the modified Mn-doped ZnS QDs was obtained. Finally, the modified Mn-doped ZnS QDs was washed three times with ethanol.

The synthesis method of MIP-coated QDs was carried out as follows. Nicosulfuron (0.1 g) was dispersed into 100 mL ethanol. Then, APTES (5 mL) was added. After stirred for 30 min, TEOS (10 mL) was added. Then, stirred for 5 min; the modified Mn-doped ZnS QDs (0.5 g) and $NH_3 \cdot H_2O$ (5 mL) were added into the mixture. After stirred for 24 h, the template was removed by Soxhlet extraction with methanol: acetic acid (19:1, *v*/*v*) until no template molecules were detected. After dried in a vacuum, MIP-coated QDs were obtained.

The non-imprinted polymer-coated Mn-doped ZnS QDs (NIP-coated QDs) were prepared using the same procedure without addition of the template nicosulfuron.

Fluorescence analysis

Fluorescence analysis was performed on an F-4600 fluorescence spectrophotometer. The spectra were observed at a wavelength in the range from 500 to 700 nm when the excitation wavelength was at the 300 nm. Slit widths (10 nm), scan speed (240 nm min^{-1}), and excitation voltage (550 V) were kept constant within each data set, and each spectrum was the average of three scans. Quartz cell (1 cm path length) was used for all measurements.

Measurements of fluorescent response to nicosulfuron

In a centrifuge tube, MIP-coated QDs or NIP-coated QDs (30 mg) were added. And the different quantity of nicosulfuron was also added. The solution pH was adjusted to 9.0 with sodium hydroxide. The constant volume was 30 mL. The fluorescence analysis was carried out after fully mixing.

In order to evaluate the potential application, the river water samples were analyzed. The 220-nm microporous membranes were used to filter water samples. The recovery study was conducted by spiking water samples with certain volume of nicosulfuron.

Results and discussion

The synthesis of MIP-coated Mn-doped ZnS QDs consists of the following steps: the preparation of Mn-doped ZnS QDs, the modification of L-cysteine, the formation of MIPs,, and elution of nicosulfuron, presented in Fig. 1.

In order to improve the luminescent properties and affinity of ZnS QDs to analyte, Mn^{2+} ions are doped into the ZnS QDs by the precipitation of Zn^{2+} with S^{2-} in the presence of Mn^{2+}. In addition, such a long lifetime makes the luminescence from the nanocrystal readily distinguished from any background luminescence.

L-Cysteine is an amino acid that has been used for synthesis of water compatible fluorescent probes. Such ligand can bind to the surface of the Mn-doped ZnS nanoparticles through the sulfur atom of the mercapto group, while the carboxylic acid group provides water compatibility.

In our experiment, APTES was used as a functional monomer. There was a strong non-covalent interaction between APTES and nicosulfuron which was necessary during the molecular imprinting process. These functional monomers (APTES) around the template (nicosulfuron) were polymerized with cross-linker (TEOS). The $NH_3 \cdot H_2O$ was chosen as a catalyst, while the L-cysteine-modified QDs were unstable in the acid environments such as acetic acid. The amino groups ($-NH_2$) in the molecules of APTES interact with the functional groups in the template molecules to form a complex through hydrogen bonding, which mainly caused the fluorescence quenching. After templates were removed from the cross linked matrix, the cavities with complementary size, shape, and orientation of functionalities were left behind.

Characterization of the MIP-coated QDs

FT-IR spectra of modified QDs and MIP-coated QDs are shown in Fig. 2a. The peaks 1635 and 1639 cm^{-1} as shown in two curves were due to C=O group which belongs to L-cysteine. In MIP-coated QDs curve, Si-O-Si asymmetric stretching was observed around 1070 cm^{-1} which was a strong and broad peak. The bands about 459 and 797 cm^{-1} were indicated by the Si-O vibrations. The bands at 3430 and 1559 cm^{-1} were N-H stretching. TEM of Mn-doped ZnS QDs and MIP-coated QDs were shown in Fig. 2b, c, respectively. The XRD of the modified QDs and the MIP-coated QDs in

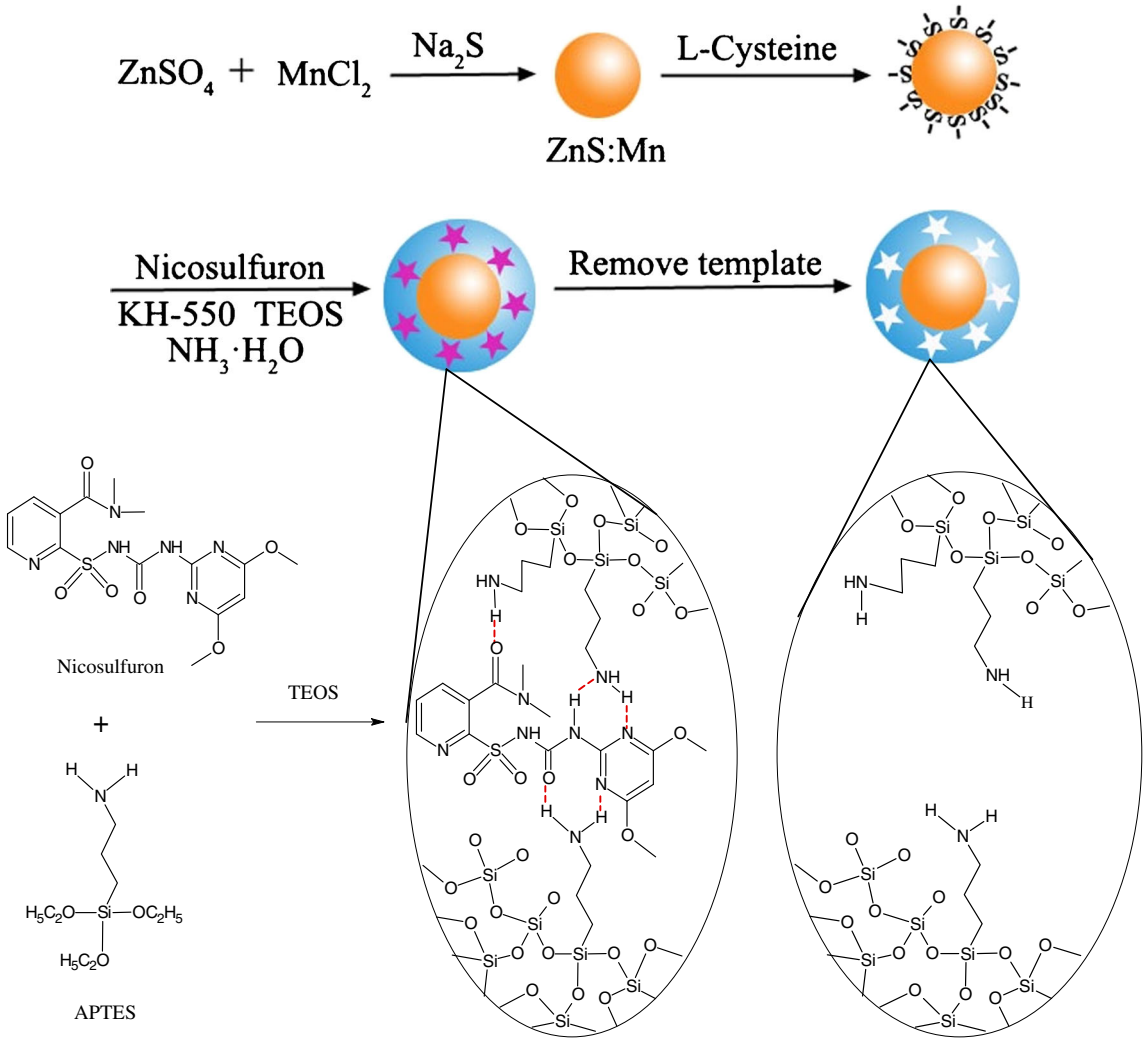

Fig. 1 The preparation process of MIP-coated QDs

Fig. 2d showed that both modified QDs and MIP-coated QDs had face-centered cubic structure. The XRD patterns of MIP-coated QDs were assigned to the (111), (220), and (311) reflections of the cubic phase Mn-doped ZnS, further suggesting the successful fabrication of MIP-coated QDs. In Fig. S2 (see ESM), dynamic light scattering measurements showed that the size of QDs and MIP-coated QDs in the present study are about 6 and 27 nm, respectively. All those showed that the MIPs were grafted on the surface of the QDs.

Fluorescence study

The excitation wavelength from 280 to 330 nm was selected to investigate the fluorescence intensity of the MIP-coated QDs. MIP-coated QDs exhibited strong fluorescence intensity at 595 nm which was obtained at the excitation wavelength of 300 nm. It is the $4T^1 \rightarrow 6A^1$ transition of the Mn^{2+} impurity that leads to the strong orange peak. Moreover, because MIP-coated QDs have very homogeneous sizes, the fluorescence intensity was very strong and the orange peak was sharp.

In order to elucidate the selectivity of the MIP-coated QDs in aqueous media, we prepared the NIP-coated QDs with the same experimental conditions as MIP-coated QDs ones without templates (nicosulfuron). Emission spectra of QDs, MIP-coated QDs, and NIP-coated QDs were illustrated in Fig. S3 (see ESM). Compared with QDs (spectrum a), the fluorescence intensity of MIP-coated QDs (spectrum c) was not only decreased but also had enough sensitivity to detect target molecule. The fluorescence of MIP-coated QDs was relatively weak before removal of templates (spectrum d). However, after simple washing with methanol and acetic acid (19:1, *v*/*v*), the fluorescence intensity of MIP-coated QDs was restored dramatically. Furthermore, the wavelength of emission has no changes, and there are no differences in overall shape of spectrum. Because the templates were removed completely from the recognition cavities in the MIP-coated QDs, the MIP-coated QDs have the similar fluorescence intensity with NIP-coated QDs (spectrum b). It indicated that MIP-coated QDs have adsorption and desorption capabilities. It suggested that MIP-coated QDs actually facilitate the application for

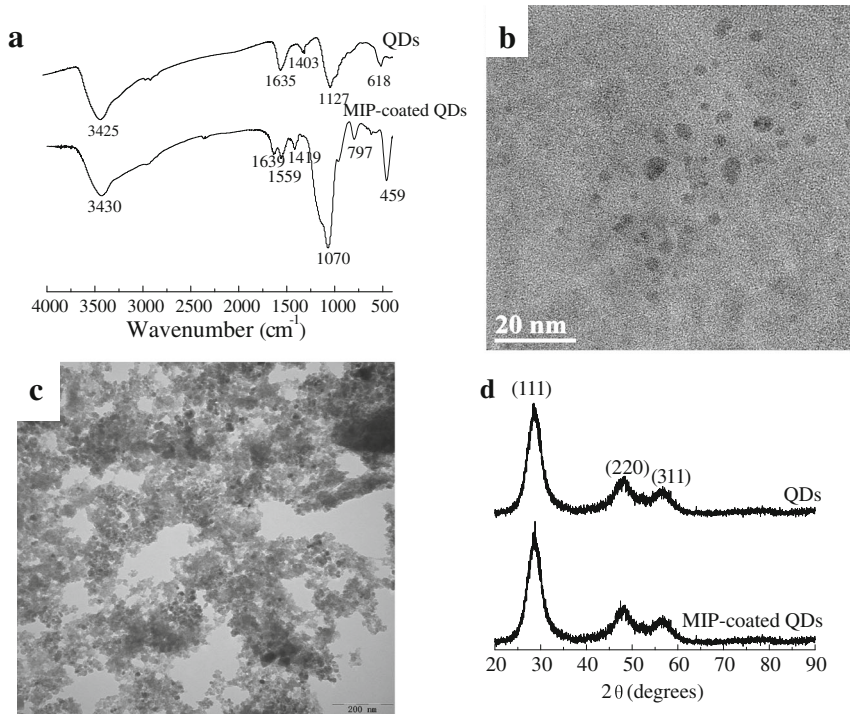

Fig. 2 Fourier transform infrared spectroscopy spectra of QDs and MIP-coated QDs, respectively (**a**), transmission electron microscope image of Mn-doped ZnS QDs (**b**), transmission electron microscope image of MIP-coated QDs (**c**), and X-ray diffraction pattern of QDs and MIP-coated QDs, respectively (**d**)

rapid and simple quantification of analytes in aqueous media without preconcentration.

The effect of pH

MIP-coated Mn-doped ZnS QDs are sensitive to chemicals in their surrounding environment including acids, bases, metallic ions, and biomolecules like proteins. The fluorescence intensity has direct correlate with pH values. In general, the fluorescence intensity of MIP-coated QDs was enhanced in alkaline medium and quenched in acidic one. The pH in the range of 4–12 was investigated to choose the optimum pH value. The pH value was adjusted by HCl and NaOH aqueous solutions. The results showed a decrease of the fluorescence intensity of MIP-coated QDs at pH lower than 7. The MIP-coated QDs and template molecule was bound through hydrogen bond. In acid medium, the hydrogen bond was decreased by hydrogen ion in solution. Moreover, under the condition of high alkaline, template molecule was hydrolyzed. The maximum fluorescence intensity of F_0/F was obtained in pH of 9. Typical evolution of fluorescence intensity versus pH for MIP-coated QDs is described in Fig. S4 (see ESM). So, the detection was carried out at pH 9.

The stable fluorescence emission measurement of MIP-coated QDs

In order to evaluate the fluorescence stability, the fluorescence emission intensity was repeatedly detected in every 5 or 10 min (Fig. S5, see ESM). This result indicates that the developed fluorescence probe possesses stability. The fluorescence intensity was maintained for 90 min because the QDs were well protected by the MIPs.

The effect of incubation time

In order to guarantee that analytes completely interact with recognition sites in the polymer matrixes, the effect of incubation time was investigated. As shown in Fig. 3, the fluorescence intensity decreased dramatically at the first stage; however, when the incubation time was 10 min, the fluorescence was slightly quenched. And the adsorption equilibrium emerged after incubation for 10 min, indicating that certain time was needed to complete the interaction. Therefore, the experiments were carried out after 10 min.

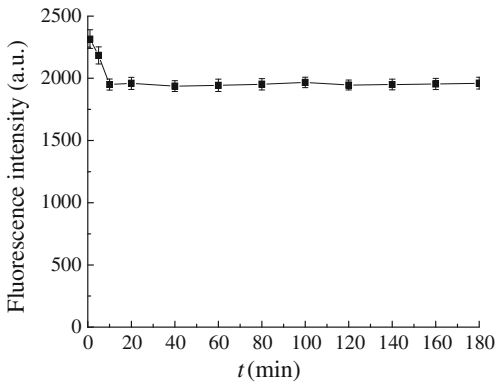

Fig. 3 Influence of incubation time on the fluorescence quenching reaction between the MIP-coated QDs and nicosulfuron (60 nmol L^{-1})

MIP- and NIP-coated QDs with template molecule of different concentrations

These MIP-coated QDs were successfully applied to the selective, sensitive, and direct fluorescence quantification of nicosulfuron in aqueous media without preconcentration and any expensive instruments. In order to prove the recognition ability of the MIP-coated QDs versus that of the NIP-coated QDs, the recognition of nicosulfuron was performed in aqueous media with different concentrations ranging from 12 to 6000 nmol L^{-1} (Fig. 4). It could be seen that the fluorescence intensity of MIP-coated QDs was quenched gradually with the increasing concentration of nicosulfuron (Fig. 4a), which indicated that nicosulfuron has been adsorbed onto the imprinted cavities conjugated with the MIPs in the MIP-coated QDs. The change of fluorescence intensity of the NIP-coated QDs (Fig. 4b) was less sensitive than that of the MIP-coated QDs with nicosulfuron. The inset in Fig. 4 exhibits the linear calibration plot of fluorescence intensity against concentration of nicosulfuron.

Selective adsorption on MIP-coated QDs

To demonstrate that the obtained MIP-coated QDs can selectively adsorb the target molecule even in a mixed system containing other molecules, we performed a selectivity study by comparing the fluorescence intensity response of the MIP-coated QDs composites to their template molecule with that to their structural analogue. The chemical structure of analogue molecule chlorimuron-ethyl was shown in Fig. S1 in the ESM. The relationship obtained for analogue chlorimuron-ethyl interacting with MIP- and NIP-coated QDs is given in Fig. 4c, d. As shown in Fig. 4a, c, the highest response to its target analyte and a lower fluorescence quenched effect to the structural analogue were observed. However, the NIP-coated QDs do not exhibit obvious difference in fluorescence intensity response between template and its structural analogue. The results suggested that MIP-coated QDs were specific to nicosulfuron but nonspecific to chlorimuron-ethyl.

As can be seen from Fig. 4, we can also find that the fluorescence quenching of NIP-coated QDs for nicosulfuron is higher than that of MIP-coated QDs for chlorimuron-ethyl. NIP-coated QDs have no imprinted cavities but have functional groups of APTES. Therefore, there existed interactions between NIP-coated QDs and nicosulfuron. Compared with chlorimuron-ethyl, nicosulfuron has more functional groups interacted with polymers. MIP-coated QDs have the special cavities to nicosulfuron. Chlorimuron-ethyl has some differences with nicosulfuron in structure, especially lack of some functional groups interacting with APTES.

Fluorescence quenching analysis

After adding the template nicosulfuron, a main reason for the fluorescence quenching was the interaction between the

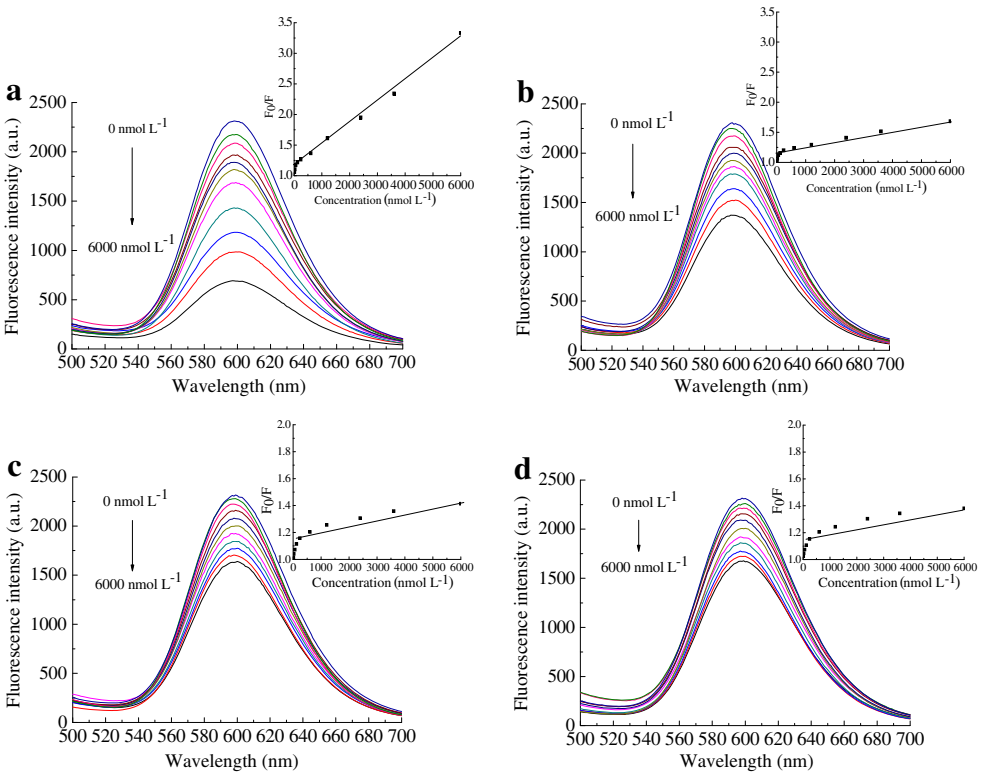

Fig. 4 Fluorescence emission spectra of MIP-coated QDs (**a**) and NIP-coated QDs (**b**) with addition of the indicated concentrations of nicosulfuron. Fluorescence emission spectra of MIP-coated QDs (**c**) and NIP-coated QDs (**d**) with addition of the indicated concentrations of chlorimuron-ethyl

template molecule and the MIP-coated QDs. The responsible fluorescence quenching mechanism of MIP-coated QDs is a charge transfer from QDs to nicosulfuron. Such charge transfer mechanism has also been reported by Tu and Liu [28] and Wang and He [29]. The UV absorption band of nicosulfuron is close to the band gap by the absorption spectra of MIP-coated QDs (Fig. S6, see ESM). These charges of the conductive bands of the QDs can transfer to the lowest unoccupied molecular orbital of the UV band of nicosulfuron. We can exclude energy transfer as a possible mechanism for fluorescence quenching because there is no spectral overlap between the absorption spectra of nicosulfuron and the emission spectrum of the MIP-coated QDs.

The data was further fitted with the Stern-Volmer equation: $(F_0/F)=1+K_{SV}[Q]$, where F_0 and F are the fluorescence intensities in the absence and presence of target molecule, respectively. $[Q]$ represents the concentration of the target molecule, and K_{SV} is the quenching constant of the target molecule. The result showed that the Stern-Volmer plots of the MIP- and NIP-coated QDs exhibited linear relationship when the concentration of nicosulfuron was changed from 12 to 6000 nmol L^{-1} (Fig. 4). K_{SV} was found to be 0.4×10^3 L mol^{-1} of MIP-coated QDs. The limit of detection (LOD), calculated by the equation $LOD=3S_b/K_{SV}$, where S_b was the standard deviation of blank measurements ($n=10$) and K_{SV} was the slope of calibration graph, was 1.1 nmol L^{-1}. The value of K_{SV} was 0.1×10^3 L mol^{-1} for NIP-coated QDs. The imprinting factor (IF) that is the ratio of the quenching constants (K_{SV}-MIP/K_{SV}-NIP) is used to evaluate the selectivity of the polymer. The result showed that the IF was 4, which is superior to the reported results [27, 30]. The imprinted sites are on the surface, so they provide excellent site accessibility and low mass transfer resistance for nicosulfuron. All these results indicated that the imprinted cavities could greatly improve the fluorescence quenching efficiency by nicosulfuron adsorption and enhance the fluorescence spectra response of MIP-coated QDs to nicosulfuron.

Application to water sample analysis

In order to evaluate the potential application of the MIP-coated QDs, the river water samples were analyzed. There are also some coexisting interferences in water samples, such as inorganic salts and trace amounts of small organic molecules. For samples, three parallel experiments were conducted. Nicosulfuron was not examined in water samples. Different concentrations of nicosulfuron (0.024, 0.24, and 2.4 μmol L^{-1}) were added into the water samples. Then, the water samples were processed according to the procedures described in section measurements of fluorescent response to nicosulfuron. The quantitative recoveries ranged from 89.6 to 96.5 %, and the relative standard deviations (RSDs) that ranged from 2.5 to 5.7 % were obtained. The results showed that the MIP-coated QDs have the potential applicability for nicosulfuron detection in real samples.

Compared with other methods reported in the literatures, this experiment results have some advantages for analyzing nicosulfuron (Table 1). As can be seen, the method index of this experiment was comparable or superable to others. When compared with chromatography methods, fluorescence analysis has unique advantages such as simplicity, low consumption, and rapidity. At the same time, because the QDs were coated with MIPs, the selectivity of fluorescence analysis was improved.

Table 1 Comparison of this method with other methods used in the literatures

Pretreatment methods	Detection methods	Samples	Analytical ranges (nmol L^{-1})	LODs (nmol L^{-1})	Recoveries (%)	RSDs (%)	Refs.
Solid phase extraction with multiwalled carbon nanotubes	HPLC-DAD	Water	0.1–97.5	0.02	87.2–100.7	2.5	[23]
Stirring extraction with PBS-methanol followed by solid phase extraction with C18	Capillary electrophoresis	Wheat Sorghum	0.02–0.12	9.36 12.96	94.1–101 92.6–93.4	5.2 6.7	[24]
Stir bar sorptive extraction with molecularly imprinted polymer	HPLC-UV	Water	25–500	0.75	93.4	1.5	[31]
Ultrasonic extraction with methanol-phosphate buffer followed by solid-phase extraction with C18	LC-MS	Soil	20–2.4×10^4	8.53×10^3	84.8–97.3	0.02–7.22	[32]
Stir bar sorptive extraction with molecularly imprinted polymer	HPLC-UV	Water	1.0–10.0	0.7	96	2.7	[33]
Solid phase extraction with C18	LC-DAD	Water	0.06–0.36	0.04	67–106	20–32	[34]
Liquid phase microextraction with hollow fiber-protected magnetized solvent-bar	HPLC-UV	Pear	2.9–290	1.0	92.1–102.9	2.1–6.8	[35]
Fluorescence probe with molecularly imprinted polymer coated quantum dots	Fluorescence spectrophotometer	Water	12–6000	1.1	89.6–96.5	2.5–5.7	This work

Conclusion

In this study, MIP-coated Mn-doped ZnS QDs were synthesized successfully. MIP-coated QDs were prepared and characterized by TEM, FT-IR, FL, and XRD. Due to application of molecular imprinting and QDs, the MIP-coated QDs have not only the high selectivity but also the strong fluorescence property. The results indicated that the MIP-coated QDs provided selectivity to nicosulfuron, which was based on the interactions of the size, shape, and functionality of the template. In addition, it has promising advantages such as simple preparation, high stability, and low cost for analysis than previous methods.

Acknowledgments This work was supported by the National Natural Science Foundation of China (No. 21205010), Fundamental Research Funds for the Central Universities (No. 2572014EB06), and Heilong Jiang Postdoctoral Funds for scientific research initiation (No. LBH-Q14001).

Conflict of interest The authors declare that they have no conflict of interests.

References

1. Turco A, Corvaglia S, Mazzotta E (2015) Electrochemical sensor for sulfadimethoxine based on molecularly imprinted polypyrrole: study of imprinting parameters. Bisoens Bioelectron 63:240–247
2. Hrichi H, Louhaichi MR, Monser L, Adhoum N (2014) Gliclazide voltammetric sensor based on electropolymerizedmolecularly imprinted polypyrrole film onto glassy carbon electrode. Sensor Actuat B 204:42–49
3. Chen LX, Xu SF, Li JH (2011) Recent advances in molecular imprinting technology: current status, challenges and highlighted applications. Chem Soc Rev 40:2922–2942
4. Song RY, Hu XL, Guan P, Li J, Zhao N, Wang QL (2014) Molecularly imprinted solid-phase extraction of glutathione from urine samples. Mat Sci Eng C 44:69–75
5. Zarejousheghani M, Fiedler P, Moser M, Borsdorf H (2014) Selective mixed-bed solid phase extraction of atrazine herbicide from environmental water samples using molecularly imprinted polymer. Talanta 129:132–138
6. Peeters M, Kobben S, Jiménez-Monroy KL, Modesto L, Kraus M, Vandenryt T, Gaulke A, Grinsven B, Ingebrandt S, Junkers T, Wagner P (2014) Thermal detection of histamine with a graphene oxide based molecularly imprinted polymer platform prepared by reversible addition–fragmentation chain transfer polymerization. Sensor Actuat B 203:527–535
7. Huang DL, Wang RZ, Liu YG, Zeng GM, Lai C, Xu P, Lu BA, Xu JJ, Wang C, Huang C (2015) Application of molecularly imprinted polymers in wastewater treatment: a review. Environ Sci Pollut Res 22:963–977
8. Lépinay S, Kham K, Millot MC, Carbonnier B (2012) In-situ polymerized molecularly imprinted polymeric thin films used as sensing layers in surface plasmon resonance sensors: mini-review focused on 2010–2011. Chem Pap 66:340–351
9. Pavlović DM, Nikšić K, Livazović S, Brnardić I, Anžlovar A (2015) Preparation and application of sulfaguanidine-imprinted polymer on solid-phase extraction of pharmaceuticals from water. Talanta 131:99–107
10. Zhou WB, Baneyx F (2014) Biofabrication of ZnS:Mn luminescent nanocrystals using histidine, hexahistidine, and His-tagged proteins: a comparison study. Biochem Eng J 89:28–32
11. Akshya S, Hariharan PS, Kumar VV, Anthony SP (2015) Surface functionalized fluorescent CdS QDs: selective fluorescence switching and quenching by Cu^{2+} and Hg^{2+} at wide pH range. Spectrochim Acta A 135:335–341
12. Yu LB, Li Z, Liu YB, Cheng F (2014) Synthesis of hierarchical TiO_2 flower-rod and application in CdSe/CdS co-sensitized solar cell. J Power Sources 270:42–52
13. Wu N, Wyart Y, Siozade L, Georges G, Moulin P (2014) Characterization of ultrafiltration membranes fouled by quantum dots by confocal lasers canning microscopy. J Membrane Sci 470: 40–51
14. Chen J, Pan JY, Du QG, Alagappan G, Lei W, Li Q, Xia J (2014) Highly efficient white quantum dot light-emitting diode based on ZnO quantum dot. Appl Phys A 117:589–591
15. Edmundson MC, Capeness M, Horsfall L (2014) Exploring the potential of metallic nanoparticles within synthetic biology. New Biotechnol 31:572–578
16. Bücking W, Massadeh S, Merkulov A, Xu S, Nann T (2010) Electrophoretic properties of BSA-coated quantum dots. Anal Bioanal Chem 396:1087–1094
17. Xu SF, Lu HZ, Li JH, Song XL, Wang AX, Chen LX, Han SB (2013) Dummy molecularly imprinted polymers-capped CdTe quantum dots for the fluorescent sensing of 2,4,6-Trinitrotoluene. Applied Materials and Interfaces 5:8146–8154
18. Zhang Z, Li JH, Wang XY, Shen DZ, Chen LX (2015) Quantum dots based mesoporous structured imprinting microspheres for the sensitive fluorescent detection of phycocyanin. Applied Materials and Interfaces 7:9118–9127
19. Rajabi HR, Farsi M (2015) Quantum dot based photocatalytic decolorization as an efficient and green strategy for the removal of anionic dye. Mat Sci Semicon Proc 31:478–486
20. Rajabi HR, Khani O, Shamsipur M, Vatanpour V (2013) High-performance pure and Fe^{3+}-ion doped ZnS quantum dots as green nanophotocatalysts for the removal of malachite green under UV-light irradiation. J Hazard Mater 250–251:370–378
21. Shamsipur M, Rajabi HR (2014) Pure zinc sulfide quantum dot as highly selective luminescent probe for determination of hazardous cyanide ion. Mat Sci Eng C 36:139–145
22. Fenoll J, Hellín P, Sabater P, Flores P, Navarro S (2012) Trace analysis of sulfonylurea herbicides in water samples by solid-phase extraction and liquid chromatography-tandem mass spectrometry. Talanta 101:273–282
23. Zhou QX, Wang WD, Xiao JP (2006) Preconcentration and determination of nicosulfuron, thifensulfuron-methyl and metsulfuron-methyl in water samples using carbon nanotubes packed cartridge in combination with high performance liquid chromatography. Anal Chim Acta 559:200–206
24. Springer VH, Aprile F, Lista AG (2014) Determination of sulfonylureas in cereal samples with electrophoretic method using ionic liquid with dispersed carbon nanotubes as electrophoretic buffer. Food Chem 143:348–353
25. Ferrer I, Thurman EM (2007) Multi-residue method for the analysis of 101 pesticides and their degradates in food and water samples by liquid chromatography/time-of-flight mass spectrometry. J Chromatogr A 1175:24–37
26. Sharma D, Nagpal A, Pakade YB, Katnoria JK (2010) Analytical methods for estimation of organophosphorus pesticide residues in fruits and vegetables: a review. Talanta 82:1077–1089
27. Liu JX, Chen H, Lin Z, Lin JM (2010) Preparation of surface imprinting polymer capped Mn-Doped ZnS quantum dots and their application for chemiluminescence detection of 4-nitrophenol in tap water. Anal Chem 82:7380–7386

28. Tu RY, Liu BH, Wang ZY, Gao DM, Wang F, Fang QL, Zhang ZP (2008) Amine-capped ZnS-Mn^{2+} nanocrystals for fluorescence detection of trace TNT explosive. Anal Chem 80:3458–3465
29. Wang HF, He Y, Ji TR, Yan XP (2009) Surface molecular imprinting on Mn-Doped ZnS quantum dots for room-temperature phosphorescence optosensing of pentachlorophenol in water. Anal Chem 81:1615–1621
30. Zhao YY, Ma YX, Li H, Wang LY (2012) Composite QDs@MIP nanospheres for specific recognition and direct fluorescent quantification of pesticides in aqueous media. Anal Chem 84:386–395
31. Yang LQ, Zhao XM, Zhou J (2010) Selective enrichment and determination of nicosulfuron in water and soil by a stir bar based on molecularly imprinted polymer coatings. Anal Chim Acta 670:72–77
32. Ye GB, Zhang W, Xin C, Pan CP, Jiang SR (2006) Determination and quantitation of ten sulfonylurea herbicides in soil samples using liquid chromatography with electrospray ionization mass spectrometric detection. Chinese J Anal Chem 34:1207–1212
33. Si BJ, Zhou J (2011) Non-hydrolytic sol–gel methodology to prepare a molecularly imprinted, organic-silica hybrid-based stir bar for recognition of sulfonylurea herbicides. Chinese J Chem 29: 2487–2494
34. Gallitzendorfer R, Timm T, Koch D, Küsters M, Gerhartz M (2011) Simultaneous determination of 12 sulfonylurea herbicides in drinking water after SPE by LC-DAD. Chromatographia 73: 813–816
35. Shi JY, Li XY, Liu C, Shao MY, Zhang HJ, Zhang HQ, Yu AM, Chen YH (2014) Determination of sulfonylurea herbicides in pears using hollow fiber-protected magnetized solvent-bar liquid-phase microextraction HPLC. Chromatographia 77:1283–1290